DOI 10.1007/s10812-022-01384-8
Journal of Applied Spectroscopy, Vol. 89, No. 3, July, 2022 (Russian Original Vol. 89, No. 3, May–June, 2022)

NEW SELECTIVE FLUORESCENT "TURN-ON" SENSOR FOR DETECTION OF Hg^{2+} BASED ON A 1,8-NAPHTHALIMIDE SCHIFF BASE DERIVATIVE

H.-L. Wu,* J.-P. Dong, F.-G. Sun, R. X. Li, and Y.-X. Jiang

UDC 535.372

A new fluorescent "turn-on" sensor for Hg^{2+}, N-allyl-4-(ethylenediamine-5-methylsalicylidene)-1,8-naphthalimide (HL) has been designed by combining a 1,8-naphthalimide moiety as a fluorophore and a Schiff base as a recognition group. As expected, HL displays high selectivity for Hg^{2+} over other ions (Na^+, K^+, Ca^{2+}, Mg^{2+}, Al^{3+}, Pb^{2+}, Fe^{3+}, Ni^{2+}, Zn^{2+}, Hg^{2+}, Ag^+, Co^{2+}, Cr^{3+}, Mn^{2+}, and Cd^{2+}) with obvious fluorescence enhancement in solution (DMF/Tris–HCl buffer, 1:1, v/v, pH 7.2). Moreover, the fluorescence intensity of HL has shown good linearity with a correlation coefficient (R^2) of 0.99, confirming that HL could be applied to quantitatively detect mercury ions in the range of 0.5–4.0 μm, whereby the detection limit reaches 0.26 μm. Meanwhile, the association constant (K_a) between Hg^{2+} and HL achieves 7.35×10^{11} M^{-1}. Based on the fluorescence titration and Job's plot analysis, the formation of a complex between HL and Hg^{2+} is by 2:1 complex ratio.

Keywords: *1,8-naphthalimide, fluorescent sensor, Hg^{2+} ion, Schiff base.*

Introduction. Mercury, which can be generated through both natural and anthropogenic activities, is a common toxicological pollutant [1, 2]. What's worse, Hg^{2+} is the only heavy metal ion that can complete the cycle of the ecosystem, and it can be converted into methylmercury by bacteria and then continuously accumulated through food chains, causing a lot of serious health issues to organisms like neurological disorders, hepatitis, nephritis, and uremia, even at very low concentrations, due to their high lipophilicity [3–7]. Therefore, it is of considerable significance, for exploring efficient, reliable, selective, and sensitive methods to monitor Hg^{2+} in the real environment.

Many modern analytic techniques such as spectrophotometry, atomic absorption spectroscopy and voltammetry have been developed to determine the concentration of Hg^{2+}, but they are not suitable for online or in-field monitoring, since their sensing operation needs fine instrumentation and sample pretreatment [8–12]. To date, the fluorescent sensor technology is believed to be an attractive and easy-to-use detection method, due to its low requirement for instrumental implementation and sample preparation [13–17]. Among them, 1,8-naphthalimide derivatives with high stability, quantum yield, large Stokes shift, and easily modified properties, have been widely used as fluorescent sensors and switchers [18–22].

In previous work, a series of fluorescent sensors based on 1,8-naphthalimide moiety to efficiently detect harmful and polluting anions and cations have been synthesized [23–35]. Based on the preceding consideration, and as a part of the continuing studies, herein, a new 1,8-naphthalimide-based fluorescent "off–on" sensor HL was designed, synthesized, and characterized for the Hg^{2+} detection, exhibiting large fluorescence, increasing with the existence of Hg^{2+}, and could be used for rapid, highly selective and sensitive detection of Hg^{2+} in the real environment.

Experimental. All chemicals and solvents used for the synthesis were obtained from commercial sources and used without further purification. Dilute hydrochloric acid or sodium hydroxide was used for tuning pH values. Tris-HCl buffer (pH 7.2) was prepared using double distilled water. The metal cation sources, $NaNO_3$, KNO_3, $CaCl_2$, $MgSO_4$, $AlCl_3$, $Pb(NO_3)_2$, $Fe(NO_3)_3{\cdot}9H_2O$, $Ni(NO_3)_2{\cdot}6H_2O$, $Zn(NO_3)_2{\cdot}6H_2O$, $Cu(NO_3)_2{\cdot}5H_2O$, $Hg(NO_3)_2{\cdot}H_2O$, $AgNO_3$, $Co(NO_3)_2{\cdot}6H_2O$, $Cr(NO_3)_3{\cdot}9H_2O$, $Mn(NO_3)_2$, and $Cd(NO_3)_2{\cdot}H_2O$ were of analytical reagent grade and were dissolved using double distilled water.

*To whom correspondence should be addressed.

School of Chemistry and Chemical Engineering at Lanzhou Jiaotong University, Lanzhou, Gansu, China; email: wuhuilu@163.com. Published in Zhurnal Prikladnoi Spektroskopii, Vol. 89, No. 3, pp. 386–393, May–June, 2022. Original article submitted April 22, 2021.

C, H, and N contents were determined using a Carlo Erba 1106 elemental analyzer. ^{1}H and ^{13}C NMR spectra were obtained with a Varian VR 400 MHz spectrometer with TMS as an internal standard. Electrospray ionization mass spectra (ESI-MS) were obtained on a BRUKER micrOTOF-Q system. The IR spectra were recorded in the 4000–400 cm^{-1} region with a Nicolet FT-VERTEX 70 spectrometer using KBr pellets. Electronic spectra were recorded on a LabTech UV Bluestar spectrophotometer. Fluorescence spectra were recorded with an F-7000 FL spectrophotometer, which had been subjected to normalized absorbance. The pH values were measured with a DELTA 320 pH meter. The melting points were measured by X-4 microscopic melting point apparatus and TLC was performed on silica gel, Fluka F60 254, 20 × 20, 0.2 mm. All the detections were carried out at 25^{o}C.

Synthesis and characterization of the sensor. Scheme 1 shows the detailed synthetic pathway of sensor HL. The intermediate products 1–2 prepared according to the procedure previously reported [36, 37].

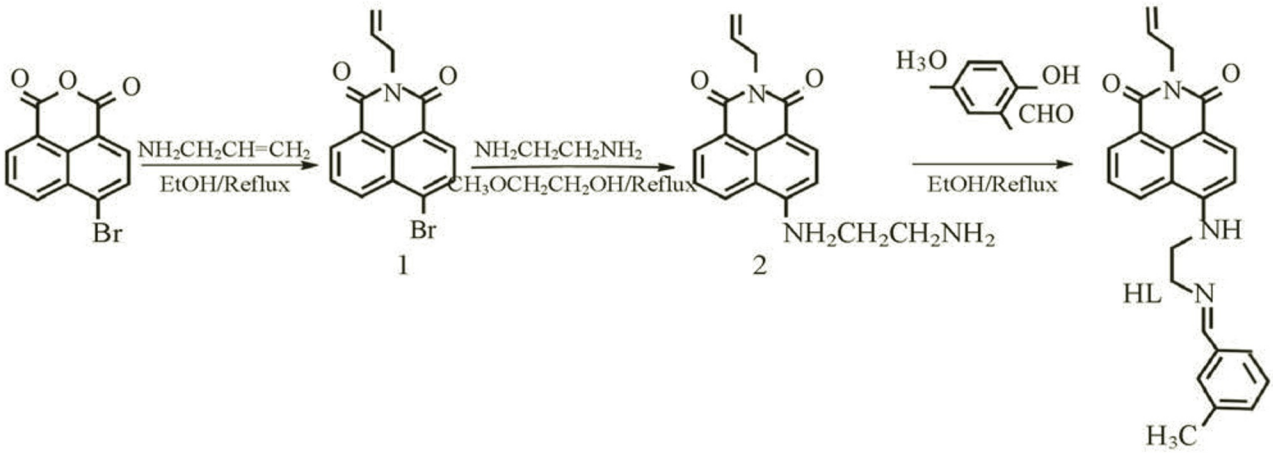

Scheme 1. Chemical structure and synthetic routine of HL.

The mixture of *N*-allyl-4-ethylenediamine-1,8-naphthalimide (2) (1 g, 3.4 mmol), 5-methylsalicylaldehyde (0.69 g, 5.1 mmol) and 40 ml of ethanol was heated to 80^{o}C for 4 h. After the mixture was cooled to room temperature, the precipitate product was filtered, washed with ethanol and dried to give 1.18 g of the final product *N*-allyl-4-(ethylenediamine-5-methylsalicylidene)-1,8-naphthalimide (HL). The progress of the reaction was monitored by TLC (the TLC eluent is dichloromethane: acetone = 1:1, R_f = 0.5). Yield: 84.3%, mp: 192–193^{o}C. Anal. calc. C 72.62; H 5.61; N 10.16%; found: C 72.38; H 5.68; N 10.19%. UV-visible (in DMF); λ/nm: 267, 328, 437. IR (KBr); *v*, cm^{-1}): 1694 (C = C), 1645 (C = N), 1572 (C = O). ESI-MS ([$C_{25}H_{23}N_3O_3$] + 1) *m*/*z* = 414.2006. ^{1}HNMR (DMSO-d_6, 400 MHz): δ (ppm) = 13.055 (*s*, 1H); δ (ppm) = = 8.682 (*d*, 1H, *J* = 8.4 Hz); δ (ppm) = 8.492 (*s*, 1H); δ (ppm) = 8.431 (*d*, 1H, *J* = 7.2 Hz); δ (ppm) = 8.259 (*d*, 1H, *J* = 8.4 Hz); δ (ppm) = 7.958 (*s*, 1H); δ (ppm) = 7.685 (*t*, H, *J* = 15.6Hz); δ (ppm) = 7.156 (*s*, 1H); δ (ppm) = 7.117 (*d*, 2H, *J* = 8.4 Hz); δ (ppm) = 6.927(*d*, 2H, *J* = 8.4 Hz); δ (ppm) = 6.768 (*d*, 1H, *J* = 8.4 Hz); δ (ppm) = 5.878–5.958 (*m*, 1H); δ (ppm) = 5.078 (*t*, 1H, 16.4 Hz); δ (ppm) = 4.623 (*d*, 2H, *J* = 4 Hz); δ (ppm) = 3.933 (*s*, 2H); δ (ppm) = 3.751 (*d*, 2H, *J* = 5.2 Hz). ^{13}CNMR (DMSO-d_6, 400 MHz): δ (ppm) = 166.80, 163.37, 162.51, 158.13, 150.64, 134.14, 133.22, 132.91, 131.39, 130.69, 129.41 128.60, 126.97, 124.33, 121.71, 120.17, 118.29, 116.14, 115.93, 107.76, 104.15, 56.82, 43.41, 41.24, 19.80.

Results and Discussion. The proposed sensor HL was characterized by elemental analysis, ^{1}H and ^{13}C NMR, UV-Vis, IR spectroscopy, and mass spectrometry. The spectral and elemental analysis data are in good agreement with its real chemical structure. HL was easily soluble in solvents like DMF, acetonitrile, tetrahydrofuran, and dichloromethane but insoluble in water.

Photophysical properties. The ability of HL to emit absorbed light energy is characterized quantitatively by the quantum yield of fluorescence Φ_F. The fluorescence quantum yield has been calculated according to

$$\Phi_F = \Phi_{ref} (S_{sample}/S_{ref}) (A_{ref}/A_{sample}) (n_{sample}/n_{ref})^2 \quad (1)$$

using *N*-butyl-4-*n*-butylamino-naphthalimide (Φ_F = 0.81 in ethanol) as a standard. Herein, Φ_F was estimated from the absorption and fluorescence spectra of HL, Φ_{ref} is the emission quantum yield of the standard, A_{ref} and A_{sample} represent

TABLE 1. Photophysical Properties of HL in Organic Solvents with Different Polarity

Solvents	λ_A, nm	ε, l·mol^{-1}·cm^{-1}	λ_F, nm	$\nu_A - \nu_F$, cm^{-1}	Φ_F
DMF	437	17761	519	3615	0.15
Acetonitrile	429	9115	519	4040	0.16
Tetrahydrofuran	426	11,403	501	3510	0.27
Dichloromethane	423	10,801	495	3440	0.13

the absorbance of the standard and sample at the excited wavelength, respectively, while S_{ref} and S_{sample} are the integrated emission band areas of the standard and sample, respectively, and n_{ref} and n_{sample} are the solvent refractive index of the standard and sample, respectively [38].

The photophysical properties of the substituted 1,8-naphthalimides are known to depend mainly on the polarization of their chromophoric system [39]. Thereby, photophysical characteristics of HL were investigated in DMF, acetonitrile, tetrahydrofuran, and dichloromethane solution. In addition, the Stokes shift ($\nu_A - \nu_F$) is an important parameter for the fluorescent compounds, indicating the difference in the properties and structures of the fluorophore between the ground state S_0 and the first excited state S_1 and has been calculated by the following equation [40, 41].

$$\nu_A - \nu_F = (1/\lambda_A - 1/\lambda_F) \cdot 10^7 \text{ cm}^{-1} . \quad (2)$$

The absorption (λ_A) and fluorescence (λ_F) maxima, the extinction coefficient (ε), the Stokes shift ($\nu_A - \nu_F$), and quantum fluorescence yield (Φ_F) of HL were presented in Table 1. The values of the quantum fluorescence yield Φ_F are in the range of ~0.13–0.27 as presented in Table 1, showing that the Φ_F of HL in polar solvents is lower than in nonpolar solvents. This fact can be explained by the photoinduced electron transfer process favored in polar solvents and the lower fluorescence emission [42]. The Stokes shift of HL is within the scope of 3,440 (dichloromethane) to 4040 cm^{-1} (acetonitrile), whereby it can be seen that the Stokes shift values are influenced by the media and it is larger in the case of polar solvents when the hydrogen bond formation or dipole–dipole interactions are favored in comparison to nonpolar media, which is in good accordance with other investigations on 1,8-naphthalimide derivatives [43, 44]. The extinction coefficient (ε) of HL ranged from 9115 to 17,761, meaning that ε is larger in polar solvents. This result can be explained in that the polarity of the organic solvents exhibits an assignable influence on ε of HL.

Investigation of the pH effect on sensing performance of HL. As the pH of the system is considered to have a significant effect on the performance of a sensor, the spectroscopic characters of HL were investigated in the pH range of 1.81–11.82. As seen from Fig. 1, the fluorescence intensity of HL is relatively stable in the range of pH from 6.37 to 10.38, implying that HL was actually pH-independent in this range and the design of HL is reasonable. Thereby, the following experiments were performed in a solution at pH 7.2.

Selectivity and interference investigation of HL. The signaling fluorescent properties of HL (10 μm) in the presence of various transition metal cations (Na^+, K^+, Ca^{2+}, Mg^{2+}, Al^{3+}, Pb^{2+}, Fe^{3+}, Ni^{2+}, Zn^{2+}, Cu^{2+}, Hg^{2+}, Ag^+, Co^{2+}, Cr^{3+}, Mn^{2+}, and Cd^{2+}) were investigated in solution (DMF/Tris-HCl buffer, 1:1, v/v, pH 7.2). As seen from Fig. 2a, it was found that only Hg^{2+} caused a significant fluorescence enhancement of HL (Φ_{Hg+HL}/Φ_{HL} = 1.84) at 526 nm among the various metal ions, suggesting a strong interaction between HL and Hg^{2+}. Furthermore, to validate the higher selectivity of HL for Hg^{2+} relative to other metal ions, the fluorescence competitive experiments of Hg^{2+} on other metal cations (Na^+, K^+, Ca^{2+}, Mg^{2+}, Al^{3+}, Pb^{2+}, Fe^{3+}, Ni^{2+}, Zn^{2+}, Cu^{2+}, Ag^+, Co^{2+}, Cr^{3+}, Mn^{2+}, and Cd^{2+}) to HL were investigated in solution (DMF/Tris-HCl buffer, 1:1, v/v, pH 7.2) and their fluorescence intensities were recorded. As shown in Fig. 2b, when excited at 430 nm, the fluorescence intensity of other potentially coexisting ions showed a similar pattern to that with only Hg^{2+}, implying that HL is a reliable and highly selective sensor for Hg^{2+} in solution (DMF/Tris-HCl buffer, 1:1, v/v, pH 7.2) and is not influenced by the subsequent addition of other competitive cations, suggesting the potential for wider use in practical application.

Fluorescence titration of HL towards Hg^{2+}. In order to obtain insight into the binding properties of HL (10 μm) with Hg^{2+}, a fluorescence titration experiment at various concentrations of Hg^{2+} was performed in solution (DMF/Tris-HCl buffer, 1:1, v/v, pH 7.2) at room temperature. As shown in Fig. 3a, upon addition of the increasing concentration gradient of Hg^{2+}, the fluorescence intensity of HL gradually increased. When the amount of Hg^{2+} added was about 5 μm,

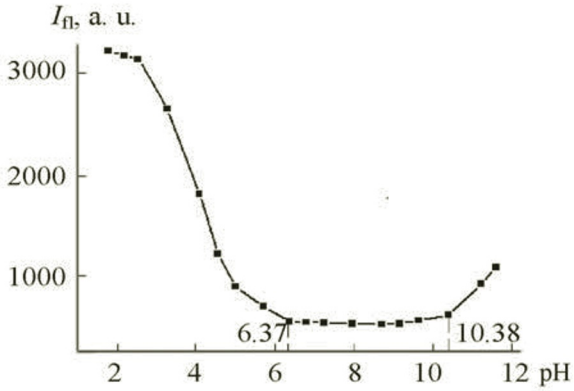

Fig. 1. Fluorescent behavior of HL at different pH values (λ_{ex} = 430 nm, 25°C).

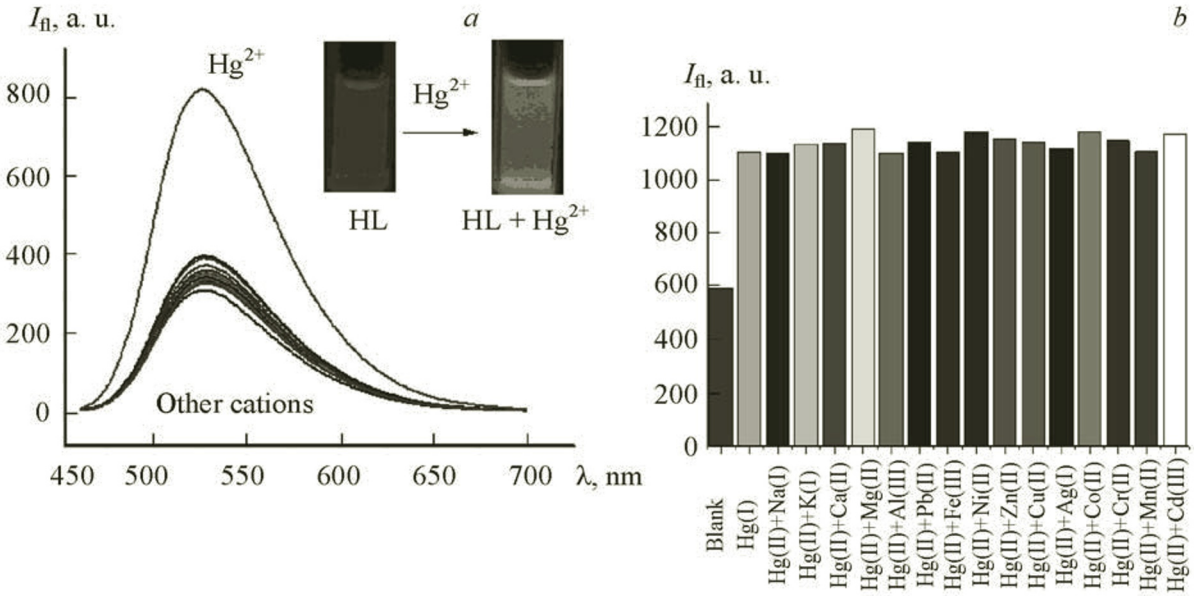

Fig. 2. a) Fluorescence spectra of HL (10 μM) in solution (DMF/Tris-HCl buffer, 1:1, v/v, pH 7.2) toward Na^+, K^+, Ca^{2+}, Mg^{2+}, Al^{3+}, Pb^{2+}, Fe^{3+}, Ni^{2+}, Zn^{2+}, Cu^{2+}, Hg^{2+}, Ag^+, Co^{2+}, Cr^{3+}, Mn^{2+}, and Cd^{2+} with an excitation at 430 nm; b) Competitive experiments in the compound HL+Hg^{2+} system with interfering metal ions at 526 nm.

the fluorescence intensity almost reached a maximum, showing negligible changes. No shifts of the emission spectra with increasing Hg^{2+} concentration observed. The nonlinear curve fitting of the fluorescence titration gives a 2:1 stoichiometric ratio between HL and Hg^{2+} (Fig. 3b). The association constant is determined by the Benesi–Hildebrand equation [45, 46]

$$\frac{1}{F - F_0} = \frac{1}{K_a(F_m - F_0)[Hg^{2+}]^n} + \frac{1}{F_m - F_0}.$$

Here, F is the fluorescence intensity at 526 nm at any given Hg^{2+} concentration, F_0 is the fluorescence intensity at 526 nm in the absence of Hg^{2+}, and F_m is the maximum fluorescence intensity at 526 nm in the presence of Hg^{2+} in solution, and n is the stoichiometric mole ratio, which is 2 in this case. The association constant K_a for L–Hg^{2+} has been calculated to be 7.35×10^{11} M^{-1} and has been evaluated graphically by plotting log $[(F - F_0)/(F_m - F)]$ against log $[Hg^{2+}]$ (Fig. 3c).

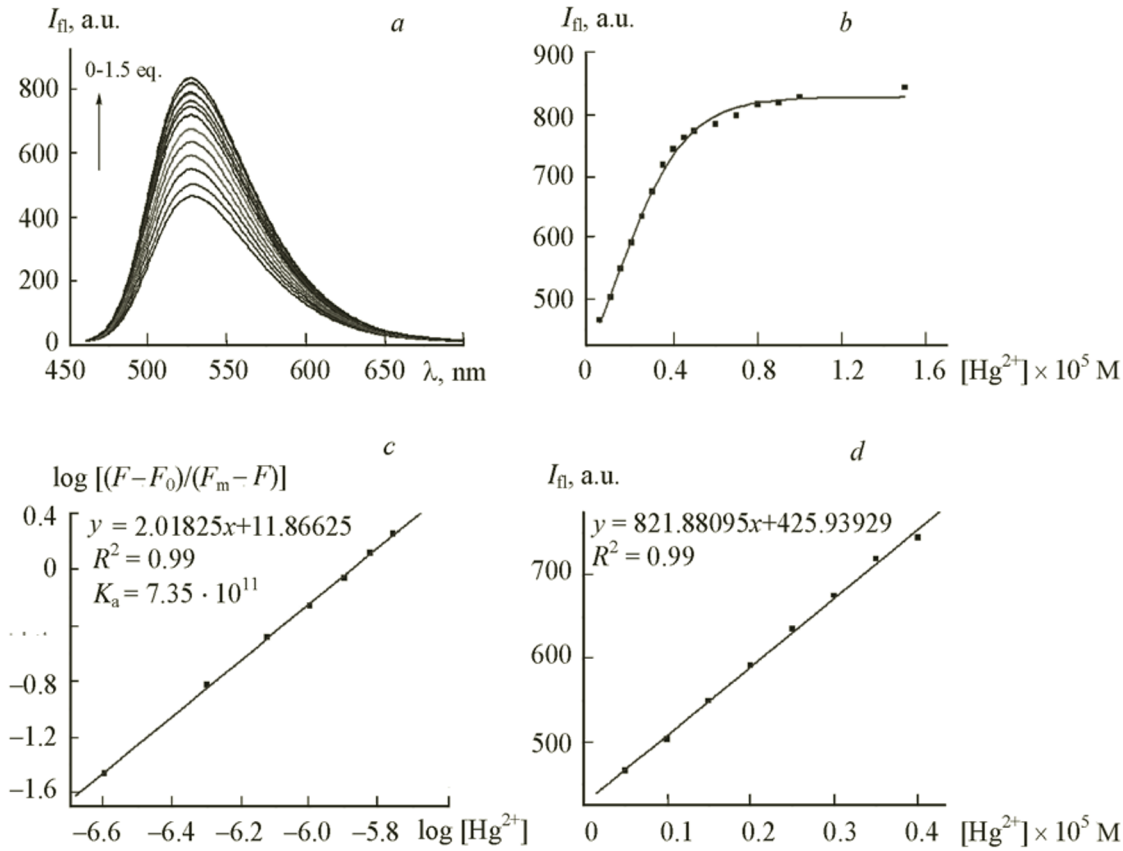

Fig. 3. a) Fluorescence titration spectra of HL with Hg^{2+} (0–1.5 eq) in solution (DMF/Tris-HCl buffer, 1:1, v/v, pH 7.2) at room temperature with an excitation of 430 nm; b) Fitting of the fluorescence titration curve of HL in solution (DMF/Tris-HCl buffer, 1:1, v/v, pH 7.2); c) Benesi–Hildebrand linear analysis plots of HL at different Hg^{2+} concentrations; d) Curve of fluorescence intensity at 526 nm of HL (1×10^{-5} M) versus increasing concentrations of Hg^{2+} (0.5–4.0 μM).

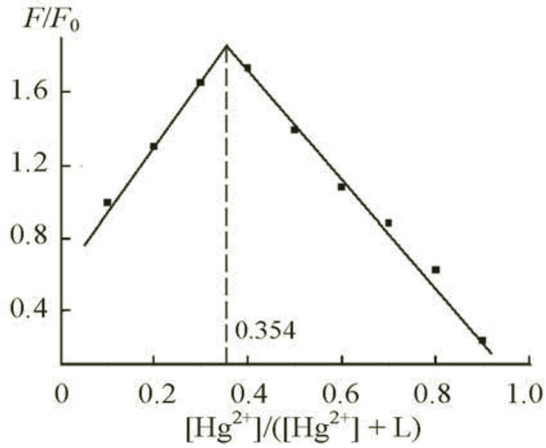

Fig. 4. Job's plot at 526 nm for determining the stoichiometry of HL and Hg^{2+} in solution (DMF/Tris-HCl buffer, 1:1, v/v, pH 7.2).

Figure 3d also displayed good linearity between the emission at 526 nm and concentrations of Hg^{2+} in the range of 0.5–4.0 μM, indicating that HL can detect quantitatively relevant concentrations of Hg^{2+}.

The detection limit (DL) based on the definition by IUPAC was calculated with the following equation [47]: DL= 3σ/*k,* where σ is the standard deviation of the blank solution, *k* is the slope of the intensity versus sample concentration. DL was calculated to be 0.26 μM, which is far below US EPA regulated limits of 31.5 μM [48]. This result confirms the ability of HL to monitor low concentrations of Hg^{2+} ions commonly encountered in both environmental and physiological systems.

Mechanism of recognition of HL towards Hg^{2+}. In spite of the stoichiometric ratio of 2:1 between HL and Hg^{2+}, obtained by the aforementioned fluorescence titration experiment, additional evidence of the exact ratio needed is provided by the Job's method. As shown in Fig. 4, the concentration of L–Hg^{2+} reached a turning point when the molar fraction of [Hg^{2+}]/[L + Hg^{2+}] was about 0.354 at 526 nm, suggesting a high binding tendency between HL and Hg^{2+} with a 2:1 stoichiometry as expected.

Based on the fluorescence titration spectra and the Job's plot, a possible binding model of HL and Hg^{2+} as shown in Scheme 1 is proposed. The fluorescence enhancement of the HL response to Hg^{2+} could be attributed to a photoinduced electron transfer (PET) [12, 49–51]. Before binding with Hg^{2+}, HL indicated moderate fluorescence intensity, probably due to the lack of a lone pair of electrons with suitable energy in the O-hydroxy Schiff base group, therefore causing sufficient intramolecular photoinduced electron transfer (PET) [52–58]. However, when HL was bound with Hg^{2+}, the PET process was blocked synchronously and the complex was more rigid, thus a significant enhancement of fluorescence was observed.

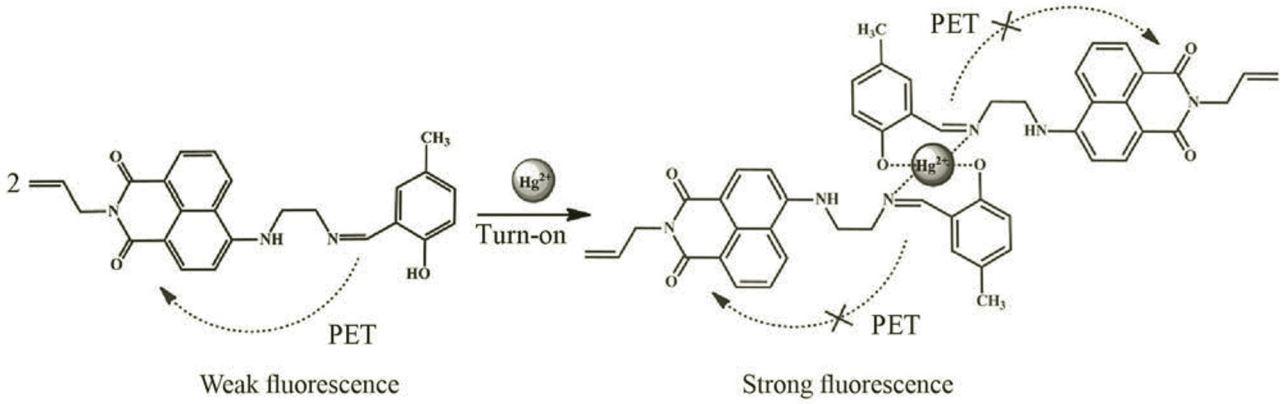

Scheme 2. Proposed binding model of HL with Hg^{2+}.

Conclusions. A new fluorescent sensor HL was designed and synthesized for detection of Hg^{2+} via fluorescence enhancement, whereby HL exhibited a high selective response to Hg^{2+} over other metal ions in solution (DMF/Tris–HCl buffer, 1:1, v/v, pH 7.2). Moreover, the binding ratio of the HL–Hg^{2+} complex was determined to be 2:1 according to the fluorescence titration and the Job's plot. The detection limit of the sensor HL toward Hg^{2+} is 0.26 μM, confirming that HL could be applied to analyze quantitatively low concentration levels of Hg^{2+} in both environmental samples and biological studies.

Acknowledgments. The present research was supported by the Foundation of a Hundred Youth Talents Training Program of Lanzhou Jiaotong University (Grant No. 152022), National Natural Science Foundation of China (Grant No. 21367017), and Natural Science Foundation of Gansu Province (Grant No. 17JR5RA090).

REFERENCES

1. M. Nendza, T. Herbst, C. Kussatz, and A. Gies, *Chemosphere*, **35**, 1875–1885 (1997).
2. I. Hoyle and R. D. Handy, *Aquat. Toxicol.*, **72**, 147 (2005).
3. A. Renzoni, F. Zino, and E. Franchi, *Environ. Res.*, **77**, 68–72 (1998).
4. L. Patrick, *Altern. Med. Rev.*, **7**, 456–471 (2002).
5. P. Grandjean, P. Weihe, R. F. White, and F. Debes, *Environ. Res.*, **77**, 165–172 (1998).
6. T. Takeuchi, N. Morikawa, H. Matsumoto, and Y. Shiraishi, *Acta Neuropathol.*, **2**, 40–57 (1962).
7. M. Harada, *Crit. Rev. Toxicol.*, **25**, 1–25 (1995).

8. I. V. Boevski, N. Daskalova, and I. Havezov, *Spectrochim. Acta B*, **55**, 1643–1657 (2000).
9. G. C. Li, G. Q. Gao, J. Y. Cheng, X. P. Chen, Y. F. Zhao, and Y. Ye, *Luminescence*, **31**, 992–996 (2016).
10. Y. L. Liu, X. Lv, Y. Zhao, M. L. Chen, J. Liu, P. Wang, and W. Guo, *Dyes Pigments*, **92**, 909–915 (2012).
11. F. Ye, X. M. Liang, K. X. Xu, X. X. Pang, Q. Chai, and Y. Fu, *Talanta*, **200**, 494–502 (2019).
12. C. B. Huang, H. R. Li, Y. Y. Luo, and L. Xu, *Dalton Trans.*, **43**, 8102–8108 (2014).
13. J. H. Hu, J. B. Li, J. Qi, and Y. Sun, *Sensor. Actuat. B: Chem.*, **208**, 581–587 (2015).
14. W. K. Dong, X. L. Li, L. Wang, Y. Zhang, and Y. J. Ding, *Sensor. Actuat. B: Chem.*, **229**, 370–378 (2016).
15. W. K. Dong, S. F. Akogun, Y. Zhang, Y. X. Sun, and X. Y. Dong, *Sensor. Actuat. B: Chem.*, **238**, 723–734 (2017).
16. Y. L. Xu, S. S. Mao, H. P. Peng, F. Wang, H. Zhang, S. O. Aderinto, and H. L. Wu, *J. Lumin.*, **192**, 56–63 (2017).
17. S. O. Aderinto, Y. L. Xu, H. P. Peng, F. Wang, H. L. Wu, and X. Y. Fan, *J. Fluoresc.*, **27**, 79–87 (2017).
18. D. Zhang, M. Li, Y. Jiang, C. Wang, Z. Wang, Y. Ye, and Y. Zhao, *Dye Pigment*, **99**, 607–612 (2013).
19. J. Wang and B. Liu, *Chem. Commun.*, **39**, 4759–4761 (2008).
20. Z. Q. Zhu, Y. Y. Su, J. Li, D. Li, J. Zhang, S. P. Song, Y. Zhao, G. X. Li, and C. H. Fan, *Anal. Chem.*, **81**, 7660–7666 (2009).
21. S. O. Aderinto, H. Zhang, H. L. Wu, C. Y. Chen, J. W. Zhang, H. P. Peng, Z. H. Yang, and F. Wang, *Color. Technol.*, **133**, 40–49 (2017).
22. W. K. Dong, Y. X. Sun, C. Y. Zhao, X. Y. Dong, and L. Xu, *Polyhedron*, **29**, 2087–2097 (2010).
23. Y. L. Xu, S. O. Aderinto, H. L. Wu, H. P. Peng, H. Zhang, J. W. Zhang, and X. Y. Fan, *Z. Naturforsch. B*, **72**, 35–41 (2017).
24. H. L. Wu, S. O. Aderinto, Y. L. Xu, H. Zhang, and X. Y. Fan, *J. Appl. Spectrosc.*, **84**, 25–30 (2017).
25. Y. Qu, C. Wang, Y. C. Wu, K. Zhao, and H. L. Wu, *J. Appl. Spectrosc.*, **87**, 429–436 (2020).
26. Y. Qu, Y. C. Wu, C. Wang, K. Zhao, and H. L. Wu, *J. Chem. Res.*, **44**, 121–127 (2020).
27. H. Zhang, Y. Qu, K. Zhao, C. Wang, Y. C. Wu, and H. L. Wu, *J. Chin. Chem. Soc.*, **67**, 1062–1069 (2020).
28. Y. Qu, Y. C. Wu, C. Wang, K. Zhao, and H. L. Wu, *Z. Naturforsch. B*, **74**, 665–670 (2019).
29. G. Z. Huang, C. Li, X. T. Han, S. O. Aderinto, K. S. Shen, S. S. Mao, and H. L. Wu, *Luminescence*, **33**, 660–669 (2018).
30. K. S. Shen, S. S. Mao, X. K. Shi, F. Wang, Y. L. Xu, S. O. Aderinto, and H. L. Wu, *Luminescence*, **33**, 54–63 (2018).
31. C. Li, X. T. Han, S. S. Mao, S. O. Aderinto, X. K. Shi, K. S. Shen, and H. L. Wu, *Color. Technol.*, **134**, 230–239 (2018).
32. H. P. Peng, K. S. Shen, S. S. Mao, X. K. Shi, Y. L. Xu, S. O. Aderinto, and H. L. Wu, *J. Fluoresc.*, **27**, 1191–1200 (2017).
33. F. Wang, Y. L. Xu, S. O. Aderinto, H. P. Peng, H. Zhang, and H. L. Wu, *J. Photochem. Photobiol. A*, **332**, 273–282 (2017).
34. H. L. Wu, H. P. Peng, F. Wang, H. Zhang, C. G. Chen, J. W. Zhang, and Z. H. Yang, *J. Appl. Spectrosc.*, **83**, 931–937 (2017).
35. S. O. Aderinto, H. Zhang, H. L. Wu, C. Y. Chen, J. W. Zhang, H. P. Peng, Z. H. Yang, and F. Wang, *Color. Technol.*, **133**, 40–49 (2017).
36. M. H. Lim, B. A. Wong, W. H. Pitcock, Jr., D. Mokshagundam, M. H. Baik, and S. J. Lippard, *J. Am. Chem. Soc.*, **128**, 14364–14373 (2006).
37. N. I. Georgiev and V. B. Bojinov, *J. Lumin.*, **132**, 2235–2241 (2012).
38. S. Roy, P. Gayen, R. Saha, T. K. Mondal, and C. Sinha, *Inorg. Chim. Acta*, **410**, 202–213 (2014).
39. K. A. Alamry, N. I. Georgiev, S. A. EI-Daly, L. A. Taib, and V. B. Bojinov, *J. Lumin.*, **158**, 50–59 (2015).
40. Y. F. Liu, M. Deng, X. S. Tang, T. Zhu, Z. G. Zang, X.F. Zeng, and S. Han, *Sens. Actuat. B: Chem.*, **233**, 25–30 (2016).
41. W. K. Dong, J. C. Ma, Y. J. Dong, L. Zhao, L. C. Zhu, Y. X. Sun, and Y. Zhang, *J. Coord. Chem.*, **69**, 3231–3241 (2016).
42. B. McLaughlin, E. M. Surender, G. D. Wright, B. Daly, and A. P. de Silva, *Chem. Commun.*, **54**, 1319–1322 (2018).
43. W. Shen, L. Q. Yan, W. W. Tian, X. Cui, Z. J. Qi, and Y. M. Sun, *J. Lumin.*, **177**, 299–305 (2016).
44. C. Y. Li, X. B. Zhang, L. Qiao, Y. Zhao, C. M. He, S. Y. Huan, L M. Lu, L. X. Jian, G. L. Shen, and R. Q. Yu, *Anal. Chem.*, **81**, 9993–10001 (2009).
45. M. Liu, L. N. Dong, A. J. Chen, Y. Zheng, D. Z. Sun, X. Wang, and B. Q. Wang, *Spectrochim. Acta A*, **115**, 854–860 (2013).
46. Z. J. Chen, L. M. Wang, G. Zou, X. M. Cao, Y. Wu, and P. J. Hu, *Spectrochim. Acta A*, **114**, 323–329 (2013).
47. L. Zhao, G. Wang, J. Chen, L. Zhang, B. Liu, J. Zhang, Q. Zhao, and Y. Zhou, *J. Fluorine Chem.*, **158**, 53–59 (2014).
48. US EPA. EPA-452/R-05-003. *Res. Triangle Park*, NC: US EPA (2005).

49. M. J. Culzoni, A. Muñoz de la Peña, A. Machuca, H. C. Goicoechea, R. Brasca, and R. Babiano, *Talanta*, **117**, 288–296 (2013).
50. H. L. Tan, B. X. Liu, and Y. Chen, *ACS Nano*, **6**, 10505–10511 (2012).
51. H. S. Lee, H. S. Lee, J. H. Reibenspies, and R. D. Hancock, *Inorg. Chem.*, **51**, 10904–10915 (2012).
52. M. Shellaiah, Y. C. Rajan, P. Balu, and A. Murugan, *New J. Chem.*, **39**, 2523–2531 (2015).
53. Y. M. Shen, Y. Y. Zhang, X. Y. Zhang, C. X. Zhang, L. L. Zhang, J. L. Jin, H. T. Li, and S. Z. Yao, *Anal. Methods*, **6**, 4797–4802 (2014).
54. L. Kang, Y. T. Liu, N. N. Li, Q. X. Dang, Z. Y. Xing, J. L. Li, and Y. Zhang, *J. Lumin.*, **186**, 48–52 (2017).
55. Q. C. Su, Q. F. Niu, T. Sun, and T. D. Li, *Tetrahedron Lett.*, **57**, 4297–4301 (2016).
56. Z. J. Chen, L. M. Wang, G. Zou, J. Tang, X. F. Cai, M. S. Teng, and L. Chen, *Spectrochim. Acta A*, **105**, 57–61 (2013).
57. Y. L. Fu, C. B. Fan, G. Liu, and S. Z. Pu, *Sens. Actuat. B: Chem*., **239**, 295–303 (2017).
58. R. H. Shen, J. J. Yang, H. Luo, B. X. Wang, and Y. L. Jiang, *Tetrahedron*, **73**, 373–377 (2017).